BIOCHEMISTRY
including biophysical chemistry & molecular biology

Article

pubs.acs.org/biochemistry

Concentration-Dependent Structural Transitions of Human Telomeric DNA Sequences

Rashid M. Abu-Ghazalah,[†] Steve Rutledge,[†] Lewis W. Y. Lau,[‡] David N. Dubins,[‡] Robert B. Macgregor, Jr.,*[,‡] and Amr S. Helmy*[,†]

[†]Edward S. Rogers Department of Electrical and Computer Engineering, Faculty of Applied Science and Engineering, University of Toronto, Toronto, Ontario, Canada

[‡]Department of Pharmaceutical Sciences, Leslie Dan Faculty of Pharmacy, University of Toronto, Toronto, Ontario, Canada

ABSTRACT: Oligodeoxyribonucleotides (ODNs) that have four repeats of the human telomeric sequence d(TTAGGG)$_n$ can assume multiple monomolecular G-quadruplex topologies. These are determined by the cation species present, the bases at the 5′ or 3′ end, and the sample preparation technique. In this work, we report our studies of the concentration dependence of the circular dichroism (CD) and the vibrational modes probed by Raman scattering of three previously characterized monomolecular G-quadruplexes: H-Tel, d[5′-A(GGGTTA)$_3$GGG-3′]; hybrid-1, d[5′-AAA(GGGTTA)$_3$GGGAA-3′]; and hybrid-2, d[5′-TTA(GGGTTA)$_3$GGGTT-3′]. At high (millimolar) ODN concentrations, we observed a transformation of the CD spectrum of H-Tel, with a relaxation time on the order of 10 h. Analysis of the kinetics of this process is consistent with the formation of an aggregated complex of folded H-Tel monomers. Upon dilution, the aggregates dissociate rapidly, yielding spectra identical to those of monomeric H-Tel. Both hybrid sequences undergo a similar transition under high-salt (1 M) conditions. The measurements suggest that for these ODN concentrations, which are typically used in high-resolution spectroscopies, the monomolecular G-quadruplex structures undergo a transition to multimolecular structures at room temperature. Guided by our findings, we propose that the terminal bases of the hybrid-1 and hybrid-2 ODNs impede the formation of these aggregates; however, in solutions containing 1 M salt, the hybrid oligonucleotides aggregate.

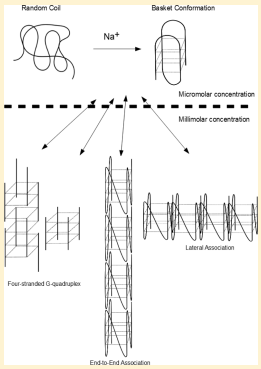

In aqueous solutions containing certain monovalent cations, guanine-rich oligodeoxyribonucleotides (ODNs) can form four-stranded structures called G-quadruplexes. The structural foundation of G-quadruplexes is the stacking of at least two G-quartets, a cyclical planar arrangement of four Hoogsteen hydrogen-bonded guanine residues.[1] The overall conformation of the quadruplex depends on several factors; these include the number and composition of the guanine and non-guanine bases in the parent oligonucleotide sequence,[2−10] the nature and concentration of cations in solution,[11,12] ligands,[13] hydration,[14−16] and the sample preparation procedure.[17]

The stoichiometry of the four-stranded species depends on the sequence of the ODN. Generally, a single cluster of guanine residues leads to the formation of a tetrameric G-quadruplex; a sequence containing two guanine-rich clusters generally yields a dimeric G-quadruplex, and a folded monomolecular G-quadruplex arises from ODNs that contain four clusters of guanine residues. However, these structures are highly polymorphic. Several other variations of their conformations have been documented.[18−20] One of the most striking examples of the possibilities afforded by their structural diversity is exhibited by d[5′-A(GGGTTA)$_3$GGG-3′], the sequence that is based on the human telomeric sequence, dGGGTTA. In the presence of sodium cations, the structure resolved by nuclear magnetic resonance (NMR) shows a monomolecular, antiparallel G-quadruplex with a basketlike topology.[21] The X-ray crystal structure of the same ODN obtained in the presence of potassium ions was found to be an all-parallel monomolecular G-quadruplex with three double-chain reversal loops.[22] However, this may not be the predominant structure in solutions containing potassium ions.[23−27]

ODNs comprised of four repeats of the human telomeric sequence but with slight modifications at the 3′ or 5′ ends displayed very different folding arrangements.[28] The most prevalent solution structure adopted by these sequences in the presence of potassium ions is (3+1). This alternative structure exhibits three strands that are oriented parallel to each other while the fourth strand is oriented in the opposite direction.[29−33] These molecules also have uncomplexed bases at the 5′ or 3′ ends that form what is known in the literature as capping structures.[30,34] Recently, a different G-rich ODN containing four repeats of the human telomeric sequence was shown to adopt an antiparallel conformation in the presence of potassium ions. Its structure is stabilized by an unprecedented two-quartet core with capping structures,[35] similar to those found in the hybrid structures.[28]

The structures formed by the longer G-rich ODNs such as H-Tel are monomolecular, and for that reason, there have been few investigations into the effect of concentration on the conformation that they adopt. However, Renčiuk et al. have

Received: May 25, 2012
Revised: August 16, 2012
Published: August 29, 2012

shown that an ODN with a sequence based on the 4-fold repeat of the human telomeric sequence partially adopts higher-order, multimolecular structures at millimolar ODN concentrations.[36] This suggests that an equilibrium state may exist between the folded monomolecular species and some unidentified aggregated species. It is not yet known whether the state of aggregation also influences the conformation of the folded monomer.

Spectroscopic techniques have proven to be very useful in the investigation of the conformational changes of G-rich ODNs. In this work, we have used circular dichroism spectroscopy (CD) and photonic crystal fiber-enhanced Raman spectroscopy to study the effect of ODN concentration and cation concentration on the conformational state of three ODNs that are known to form folded quadruplex structures. The CD signal is diagnostic of the overall structure adopted by the ODN; this method can report subtle changes in conformation and has been widely used to study biomolecules. The newly developed PCF-enhanced Raman spectroscopy played a pivotal role in elucidating the conformational states for small-volume samples at low laser powers.[37] Nonresonant Raman spectroscopy has not been customarily useful for the study of solutions to date because of the low signal-to-noise ratio obtained at nonthermally destructive laser powers, yet it is a powerful method for studying the structures of molecules in solution. The advantage of the photonic crystal fiber-enhanced Raman spectroscopy reported here is that it requires laser powers below the specimen damage threshold to provide useful Raman spectra for samples without the need for enhancement techniques such as surface enhancement using plasmonics.

We report here the effect of ODN strand concentration on the topology and state of aggregation of three oligonucleotides that are based on the human telomeric sequence. The biochemical and biophysical characterization of H-Tel and other four-stranded ODNs has relied on many different techniques that are performed at DNA concentrations ranging from submicromolar to several millimolar. However, through analysis of the concentration dependence of equilibrium states and the time dependence of the conformational changes, the data we present here clearly show that there is a reversible equilibrium that involves the aggregation of the monomers of H-Tel. At millimolar concentrations, the equilibrium favors an aggregated species that is not present at lower concentrations. The presence of aggregated monomers means that direct comparison of the results of different biochemical techniques that employ widely different concentrations ranges may not be valid. In addition to the intrinsic interest in the demonstration of a previously unidentified equilibrium involving the single molecules of the oligonucleotide H-Tel, our data have important implications for the interpretation of much of the data used in the characterization of this molecule.

MATERIALS AND METHODS

Oligonucleotides. The cartridge-purified oligonucleotides listed in Table 1 were purchased from ACGT DNA Technologies Corp. (Toronto, ON). They were dissolved in and dialyzed against Optima Water purchased from Fisher Scientific. The dialyzed DNA samples were lyophilized and stored at −20 °C. All samples were then redissolved in 10 mM Tris-HCl (pH 7.5) (Bio-Rad Laboratories, Hercules, CA) with 0.1 or 1 M KCl or NaCl (Sigma-Aldrich, St. Louis, MO) for experimentation. All samples were left at ambient temperature for a predetermined time (see Results). The concentrations of the ODNs were determined spectrophotometrically using extinction coefficients at 260 nm calculated according to the nearest-neighbor model.[38]

Table 1. Oligonucleotides Used in These Experiments

name	sequence	ε, extinction coefficient (M^{-1} cm^{-1})
TG4T	d(5′-TGGGGT-3′)	64840
H-Tel	d(5′-AGGGTTAGGGTTAGGGTTAGGG-3′)	255320
Hyb-1	d(5′-**AAA**GGGTTTAGGGTTAGGGTTAGGG**AA**-3′)	316120
Hyb-2	d(5′-**TTA**GGGTTAGGGTTAGGGTTAGGG**TT**-3′)	288920

Circular Dichroism Spectroscopy. CD spectra were recorded at 25 °C in 1.0 nm increments from 220 to 300 nm with an Aviv (Lakewood, NJ) model 62A DS circular dichroism spectrometer using a cuvette with a 0.1 cm path length for ODN strand concentrations of 20 μM or a 0.001 cm path length for strand concentrations of 2 mM. The CD spectra presented are the average of three consecutively measured scans.

Kinetics of Association. Samples of the human telomeric sequence [H-Tel (Table 1)], ranging in concentration from 3 to 7 mM, were dissolved in 10 mM Tris-HCl (pH 7.5) and 1 M NaCl (t = 0). The solution was then vortexed, degassed, and loaded into the 0.001 cm path length two-piece cuvette. The cuvette was sealed with wax to prevent evaporation of the sample. It is estimated that the time between the addition of the buffer to the sample and the acquisition of the first point (the dead time) did not exceed 5 min. The changes in ellipticity at 25 °C were monitored at 258 nm and fit to one or two exponentials to obtain the relaxation time(s), τ, of the conformational change.

Raman Spectroscopy. A hollow-core photonic crystal fiber (PCF, model HC800), purchased from Crystal Fiber, was prepared as described previously.[39] The PCF is a novel optical tool that features a hollow core surrounded by a cladding composed of silica and air.[40] A sample volume of 10 μL containing 2 mM DNA strands was transferred into the fiber by capillary action by immersing one end of the tube in the solution contained in a small well. The fiber and well were then placed on a JY Horiba (Boston, MA) HR800 LabRam system for Raman excitation and collection. The Raman system included a 4 mW HeNe laser emitting at a wavelength of 633 nm. The beam was directed onto the sample by a dielectric filter used as a dichroic mirror with a drop-off Stokes edge of <150 cm^{-1}. Light was coupled into the core of the PCF through a 100× objective with a numerical aperture of 0.90. Backscattered radiation from the entire length of the PCF was collected through the same objective. The collected radiation was refocused and passed through the dielectric filter, after which it was directed through an adjustable slit aperture into the spectrometer. The slit aperture was kept at 500 μm throughout the experiment. The spectrometer was 300 mm in length and incorporated a grating with 1800 lines/mm, which provided a resolution of 2.4 cm^{-1}/pixel. Raman signal was detected using a 16 bit Peltier-cooled 1024 × 256 pixel CCD. Acquisition times of 10 s were consistently used, and the signal was averaged over 10 cycles. Additionally, the system was equipped with a motorized XY stage with a resolution of 0.1 μm that allows optimal alignment of the objective and the PCF.

For accurate analysis, the background contribution arising from the instrument was removed and Gaussian−Lorentzian curves were fit to modes of interest. The intensity of all spectra was normalized to the 1092 cm^{-1} mode of the phosphodiester backbone of DNA.

RESULTS

CD Spectroscopy. As a point of reference, Figure 1 displays the CD spectrum of a solution of d(TG_4T) in a buffer

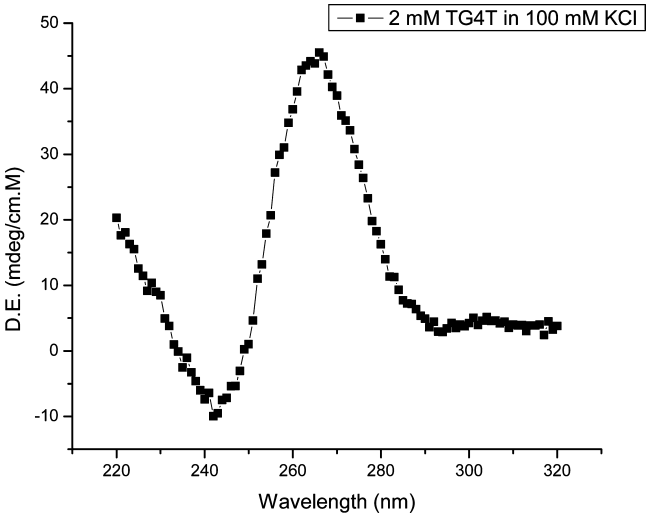

Figure 1. CD spectrum of 2 mM d(TG_4T) in 10 mM Tris-HCl (pH 7.5) and 100 mM KCl at 25 °C.

containing 100 mM KCl. This ODN forms a well-defined tetrameric G-quadruplex in the presence of either sodium or potassium cations.[41,42] The CD spectrum displays a positive band around 260 nm and a negative band around 240 nm, characteristic features of the CD spectra of parallel-stranded G-quadruplexes.[43]

The solution structure of H-Tel (Table 1), resolved using NMR, was shown to be a monomolecular antiparallel G-quadruplex that adopts a basket conformation.[21] The CD spectrum of this ODN in the presence of sodium cations gave a positive band around 290 nm and a negative band around 260 nm.[44] In panels A and B of Figure 2, we compare the CD spectra of H-Tel at low (20 μM) and high (2 mM) strand concentrations after incubation for 24 and 48 h, respectively. After incubation for 24 h in the absence of any added Na^+, the spectrum of 20 μM H-Tel shows a small positive peak around 255 nm. When the strand concentration was increased to 2 mM, we observed a similar positive band around 258 nm and a shoulder at ∼295 nm (Figure 2A). Increasing the incubation time to 48 h did not result in any change to the CD spectrum of the 20 μM sample. The CD spectrum of 2 mM H-Tel changed slightly after a 48 h incubation; the positive peak at 258 nm became less intense, and the intensity of the shoulder at ∼295 nm increased slightly.

As shown in panels A and B of Figure 2, the spectroscopic changes were much larger following incubation in the presence of sodium ions. The CD spectrum of 20 μM H-Tel in the presence of 100 mM or 1 M NaCl consistently displays characteristics of an antiparallel G-quadruplex: a peak around 290 nm and a trough around 260 nm.[43] The spectra remain unchanged after incubation for 24 and 48 h with a slight increase in the intensity of the band at 295 nm in the sample containing 1 M NaCl.

The spectral properties of 2 mM H-Tel in solutions containing 0.1 or 1 M NaCl differ markedly from those of the 20 μM samples. At either salt concentration, the CD spectrum of 2 mM H-Tel shows an intense peak around 258 nm and a band with a considerably reduced intensity around 290 nm (Figure 2A,B). This spectrum qualitatively resembles that of the all-parallel G-quadruplex formed by TG_4T (Figure 1) without the shoulder at 290 nm. The CD spectrum of 2 mM H-Tel in the presence of 1 M NaCl remains the same after a 48 h incubation. In contrast, the spectrum of 2 mM H-Tel in a 0.1 M NaCl solution exhibits a slightly more intense 258 nm band and a small reduction in the intensity of the 290 nm shoulder after the longer incubation (Figure 2A,B).

We also investigated the effect of concentration on the spectroscopic characteristics of Hyb-1 and Hyb-2, which are variants of H-Tel (Table 1). In the presence of K^+, Hyb-1 and Hyb-2 adopt a monomolecular 3+1 configuration called hybrid-1 and hybrid-2, respectively.[30,31] Panels A and B of Figure 3 compare the CD spectra of Hyb-1 at low (20 μM) and high (2 mM) ODN concentrations following incubation for 24 and 48 h, respectively. From these figures, it can be seen that in the absence of any added KCl, the dilute sample displays a single positive band around 255 nm, which is similar to the spectrum of H-Tel under this condition. However, at the higher ODN concentration, the CD spectrum of Hyb-1 displays a broad peak

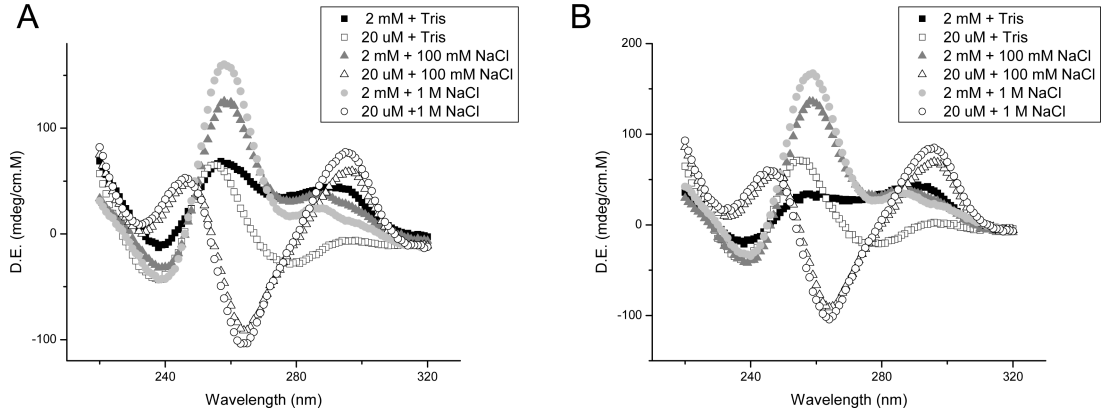

Figure 2. CD spectra of 20 μM and 2 mM H-Tel in 10 mM Tris-HCl (pH 7.5) (squares) with either 100 mM NaCl (triangles) or 1 M NaCl (circles) incubated for 24 (A) or 48 h (B) at 25 °C.

dx.doi.org/10.1021/bi300689t | Biochemistry 2012, 51, 7357−7366

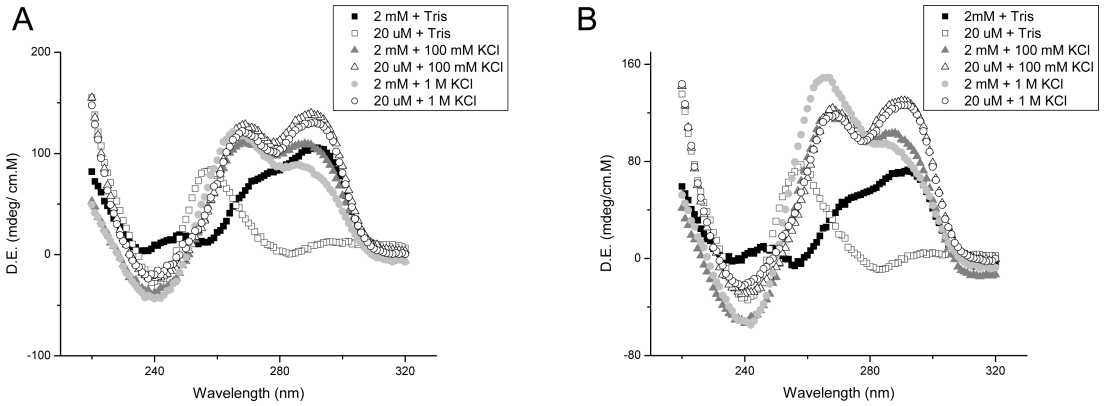

Figure 3. CD spectra of 20 μM and 2 mM Hyb-1 in 10 mM Tris-HCl (pH 7.5) (squares) with either 100 mM NaCl (triangles) or 1 M NaCl (circles) incubated for 24 (A) or 48 h (B) at 25 °C.

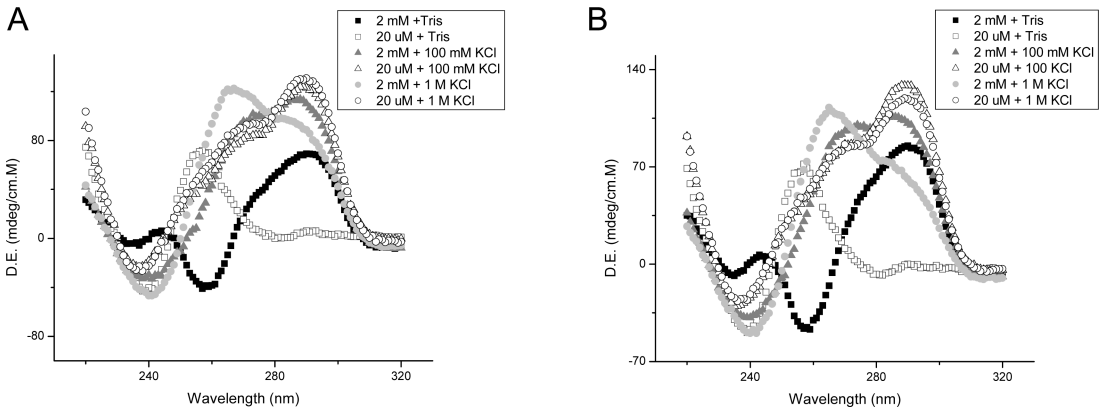

Figure 4. CD spectra of 20 μM and 2 mM Hyb-2 in 10 mM Tris-HCl (pH 7.5) (squares) with either 100 mM NaCl (triangles) or 1 M NaCl (circles) incubated for 24 (A) or 48 h (B) at 25 °C.

with a maximum at ~290 nm; the intensity of this peak decreases gradually at shorter wavelengths (Figure 3A,B). In solutions containing 100 mM KCl, the CD spectra are qualitatively similar and independent of the ODN concentration with positive peaks at ~270 and ~290 nm. These spectra resemble the CD spectrum of hybrid-1 structures[29] (Figure 3A,B). At 2 mM, we observed a modest increase in the intensity of the band at 270 nm relative to that of the peak at 290 nm after the 48 h incubation (Figure 3B). In the presence of 1 M KCl, only the 2 mM Hyb-1 sample displayed a change in its CD spectral features; the spectrum of the 20 μM sample remained unchanged (Figure 3A). At higher ODN and KCl concentrations, we observed a decrease in the intensity of the 290 nm band after 24 h (Figure 3A); after 48 h, the intensity of the band at around 270 nm increased and was slightly blue-shifted (Figure 3B).

The behavior of Hyb-2 was quite similar to that of Hyb-1. At 20 μM and in the absence of added salt, the spectrum of Hyb-2 exhibited a single positive peak around 255 nm (Figure 4A,B), a behavior similar to that of H-Tel and Hyb-1 (Figures 2A,B and 3A,B, respectively). The CD spectrum of 2 mM Hyb-2 (Figure 4A,B) in the absence of added salt resembles that of Hyb-1 (Figure 3A,B) with the addition of a trough around 260 nm. In solutions containing 100 mM KCl, the 20 μM and 2 mM Hyb-2 samples displayed spectra that are alike and that correspond to the hybrid-2 structure[28] (Figure 4A). The spectra of these remained essentially unchanged following incubation for 48 h with a slight deviation for the 2 mM sample (Figure 4B). The CD spectra of 20 μM Hyb-2 in 1 M KCl at 24 and 48 h (panels A and B of Figure 4, respectively) resemble the spectrum of Hyb-2 in 100 mM KCl. Larger differences were observed for the 2 mM sample in the presence of 1 M KCl. A positive peak appeared around 260 nm with a prominent shoulder around 295 nm. The spectra remained qualitatively the same at the 24 and 48 h marks (Figure 4A,B).

Kinetics of the Conformational Transition of H-Tel at High ODN Concentrations. Panels A and B of Figure 2 show that there is a time-dependent change in the CD spectrum of H-Tel in the presence of salt. We monitored the time course of the change in the CD signal at 258 nm for solutions containing 3−7 mM ODN and 1 M NaCl. We used 1 M Na^+ instead of 0.1 M to accelerate the conformation change and to allow us to monitor the structural changes in a reasonable time frame. Panels A and B of Figure 2 show that the CD spectra of H-Tel at 1 M and 100 mM Na^+ are qualitatively similar, suggesting that the solution structures at both ionic strengths are also similar.

The relaxations we observed at 258 nm were biexponential except at the highest concentration, at which it was monoexponential. The relaxation times are concentration-dependent; thus, it is not a monomolecular process that we are observing. However, the range of concentrations over which we could observe relaxations precluded analysis of the kinetics of the process. Therefore, these data provide an only qualitative analysis of the processes we monitored. Figure 5 displays the

dx.doi.org/10.1021/bi300689t | *Biochemistry* 2012, 51, 7357−7366

dependence of the relaxation times (τ) on the concentration of H-Tel.

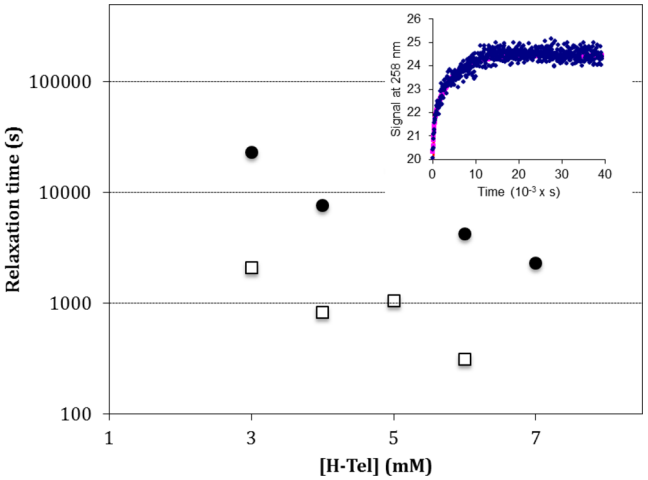

Figure 5. Concentration dependence of the two relaxation times observed at high concentrations of H-Tel. At 7 mM H-Tel, the data were fit best with a single exponential. The inset shows a typical relaxation curve obtained by measuring the magnitude of the CD signal at 258 nm.

The very slow transition displayed by Hyb-1 and Hyb-2 sequences even in the presence of 1 M KCl prevented us from measuring the kinetics of the structural transition. To accelerate the process, we heated these samples to 90 °C and then cooled them to room temperature. The CD spectra we obtained after this treatment resembled that of H-Tel at millimolar strand concentrations, suggesting that Hyb-1 and Hyb-2 adopt a conformation similar to that of H-Tel at high concentrations.

Raman Spectroscopy. Raman spectroscopy was used to determine the formation of G-quadruplex structures and to monitor changes in the conformations of the guanine residues (*syn*/*anti*) involved in G-quartet formation. Solutions of DNA samples (2 mM strands) were loaded into photonic crystal fibers (PCFs) to provide an enhancement to the Raman signals by means of total internal reflection and the photonic bandgap effect. Figure 6 shows the spectra of the four DNA sequences (Table 1) in the presence of 100 mM NaCl for H-Tel or 100 mM KCl for TG_4T, Hyb-1, and Hyb-2, after a 48 h incubation at 25 °C. All Raman modes were calibrated using the phosphate mode at 1092 cm^{-1} as a reference.[45]

The Raman spectrum of TG_4T (Figure 6a) was collected as a reference because it is known to assume a tetramolecular G-quadruplex with the guanine residues forming G-quartets assuming the *anti* conformation. In a Raman spectrum, the marker for Hoogsteen hydrogen bonds, and hence the formation of G-quartets, is the band at 1480.2 cm^{-1} arising from the C8═N7-NH2 vibrational mode.[45] The intense mode at 685.5 cm^{-1} and the much less intense mode at 670 cm^{-1} are consistent with the majority of glycosidic angles of the guanine residues being in the *anti* conformation.[45,46] The Raman spectrum of H-Tel in 100 mM NaCl after an incubation period of 48 h is shown in Figure 6b. It displays an intense band around 1481 cm^{-1} confirming the presence of a G-quadruplex structure, and it also exhibits an intense mode at 686.8 cm^{-1} and a shoulder at 667.6 cm^{-1}, suggesting that the majority of the guanines are in the *anti* glycosidic conformation.[45]

Similarly, the Raman spectra of Hyb-1 and Hyb-2, after a 48 h incubation period in the presence of 100 mM KCl (panels c and d of Figure 6, respectively), display intense modes at 1481 cm^{-1}, confirming the presence of G-quadruplexes. Both spectra display a strong guanine *anti* mode around 684 cm^{-1} with a small shoulder mode around 667 cm^{-1}.

We monitored the rate of conversion between the *anti* (~685 and ~1335 cm^{-1}) and *syn* (~670 and ~1325 cm^{-1})[45,46] conformations by collecting the Raman spectra of H-Tel, Hyb-1, and Hyb-2 as a function of time, with time zero being the moment at which buffer containing 100 mM cation (Na^+ or K^+) was added to the lyophilized samples (Figure 7). From these results, it is clear that over the course of 48 h the intensities of the *syn* guanine Raman modes of H-Tel around 670 and 1325 cm^{-1} decrease with time in relation to those corresponding to guanine *anti* modes around 685 and 1333 cm^{-1}. In contrast, neither the Hyb-1 nor the Hyb-2 Raman spectrum displays time-dependent changes in intensity of the modes corresponding to the *anti* and *syn* conformations in relation to one another, signaling that these ODNs do not undergo significant conformational changes in 100 mM KCl.

DISCUSSION

Circular dichroism spectroscopy is a powerful technique for monitoring changes in the secondary structure of proteins and nucleic acids. Applied to the analysis of G-quadruplex structure, CD spectroscopy is often used to differentiate between antiparallel and parallel strand arrangements within a G-quadruplex. Generally, a CD spectrum of guanine-rich ODNs with a positive peak around 260 nm and a trough around 240 nm is ascribed to a parallel-stranded G-quadruplex. On the other hand, a spectrum having a positive Cotton effect around 295 nm and a trough around 260 nm is considered to correspond to an antiparallel G-quadruplex. Two groups have shown these spectral features arise from the orientation of the stacked adjacent G-quartets.[47,48] In addition to differentiating between two topologies, CD spectroscopy affords a convenient route to measure the kinetics of the changes in secondary structures, ligand binding, and other structural changes. In what follows, we combine the data from CD spectroscopy and those obtained from nonresonant Raman spectroscopy in photonic crystal fibers. This newly developed technique of conducting Raman spectroscopy in photonic crystal fibers enhances the detected Raman signals. In turn, it allows us for the first time to study the effects of DNA strands as a function of their concentration for three types of G-quadruplex-forming ODNs that are based on the human telomeric sequence.

For most of the measurements presented here, we have used two different concentrations of oligodeoxyribonucleotides, 0.02 and 2.0 mM. The lower concentration was chosen because it is within the range of the spectroscopic methods typically used in UV absorbance and circular dichroism using conventional laboratory apparatus. This is a concentration in line with those used in most physical and biochemical measurements of these structures. We chose the higher concentration (2 mM) for two reasons. It is in the range of concentrations used in structural studies that employ magnetic resonance and because it was the lowest concentration that would permit us to conduct the kinetics experiments at 25 °C within a reasonable time frame (<36 h). The conformational transitions were not complete at lower ODN concentrations (0.6 and 1.5 mM) after 36 h. Below 0.6 mM, we did not observe any time-dependent signal change even after incubation for 48 h, which we presume indicates that

dx.doi.org/10.1021/bi300689t | *Biochemistry* 2012, 51, 7357−7366

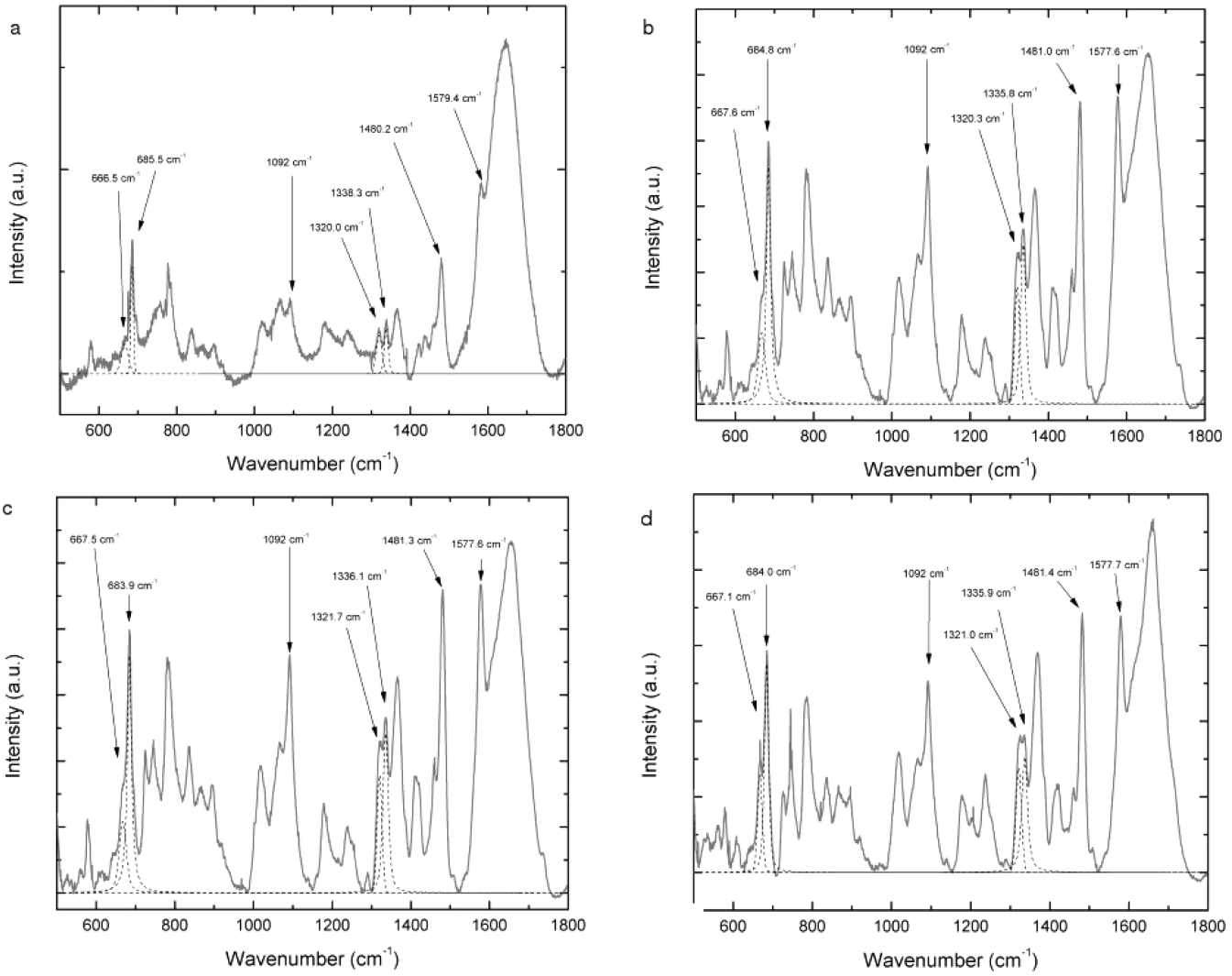

Figure 6. Raman spectra of d(TG_4T) in 10 mM Tris-HCl and 100 mM KCl (a), H-Tel in Tris-HCl and 100 mM NaCl (b), Hyb-1 in 10 mM Tris-HCl and 100 mM KCl (c), and Hyb-2 in 10 mM Tris-HCl and 100 mM KCl (d). All samples contained 2 mM ODN and were incubated for 48 h at 25 °C.

H-Tel remains a folded monomolecular G-quadruplex. The optical densities of the 2 mM and 20 μM samples are approximately 0.5 based on an extinction coefficient of 255320 M^{-1} cm^{-1} and pathlengths of 0.01 and 1 mm, respectively.

Figures 2−4 show that in the absence of added salt, the CD spectra of the samples at the lower concentration (20 μM) resemble those of guanine-rich ODNs that contain 7-deaza-8-azaguanine residues, which are assumed to be unfolded.[37] In contrast, when we increased the ODN concentration 100-fold to 2 mM, the CD bands around 260 and 295 nm suggest that a fraction of the ODNs exist in the G-quadruplex conformation. The signal around 260 nm becomes less pronounced for H-Tel after the 48 h incubation (Figure 2A,B). In the absence of any added salt, 2 mM solutions of Hyb-1 and Hyb-2 appear to adopt a mixture of conformations. The CD spectrum of Hyb-2 displayed a trough around 260 nm, suggesting that antiparallel G-quadruplex structures are more prevalent than the parallel topologies for that sequence under these conditions (Figure 4A,B).

The CD spectrum of H-Tel (Figure 2A,B) displays a striking dependence on the concentration of the ODN. At micromolar ODN concentrations in either 100 mM or 1 M NaCl, the spectrum of H-Tel resembles that of antiparallel G-quadruplexes,[49] while at higher ODN concentrations, the spectrum has features, such as a positive band at 258 nm, that resemble those of parallel-stranded G-quadruplexes (Figure 1). In addition to the band at 258 nm, there is a shoulder around 290 nm that might denote the presence of the antiparallel basket conformation for the H-Tel sequence in the presence of Na^+ [21] (Figure 2A,B). From this, it appears that at millimolar concentrations H-Tel exists as a mixture of parallel structure(s) and antiparallel species, with the former being more prevalent. Furthermore, the shoulder at 290 nm is less intense in the presence of 1 M NaCl than the shoulder observed in the spectrum of 2 mM H-Tel in 100 mM NaCl (Figure 2A). However, the intensity of the CD signal at 290 nm for the 2 mM H-Tel spectrum in 100 mM Na^+ becomes comparable to that of this ODN in 1 M NaCl after 48 h (Figure 2B). This indicates that the rate of structural conversion of H-Tel at higher oligonucleotide concentrations increases with increasing NaCl concentration as previously described by Neidle and Balasubramanian.[50]

The time-dependent changes in the intensity of the Raman modes corresponding to the *anti* and *syn* conformations in the

dx.doi.org/10.1021/bi300689t | *Biochemistry* 2012, 51, 7357−7366

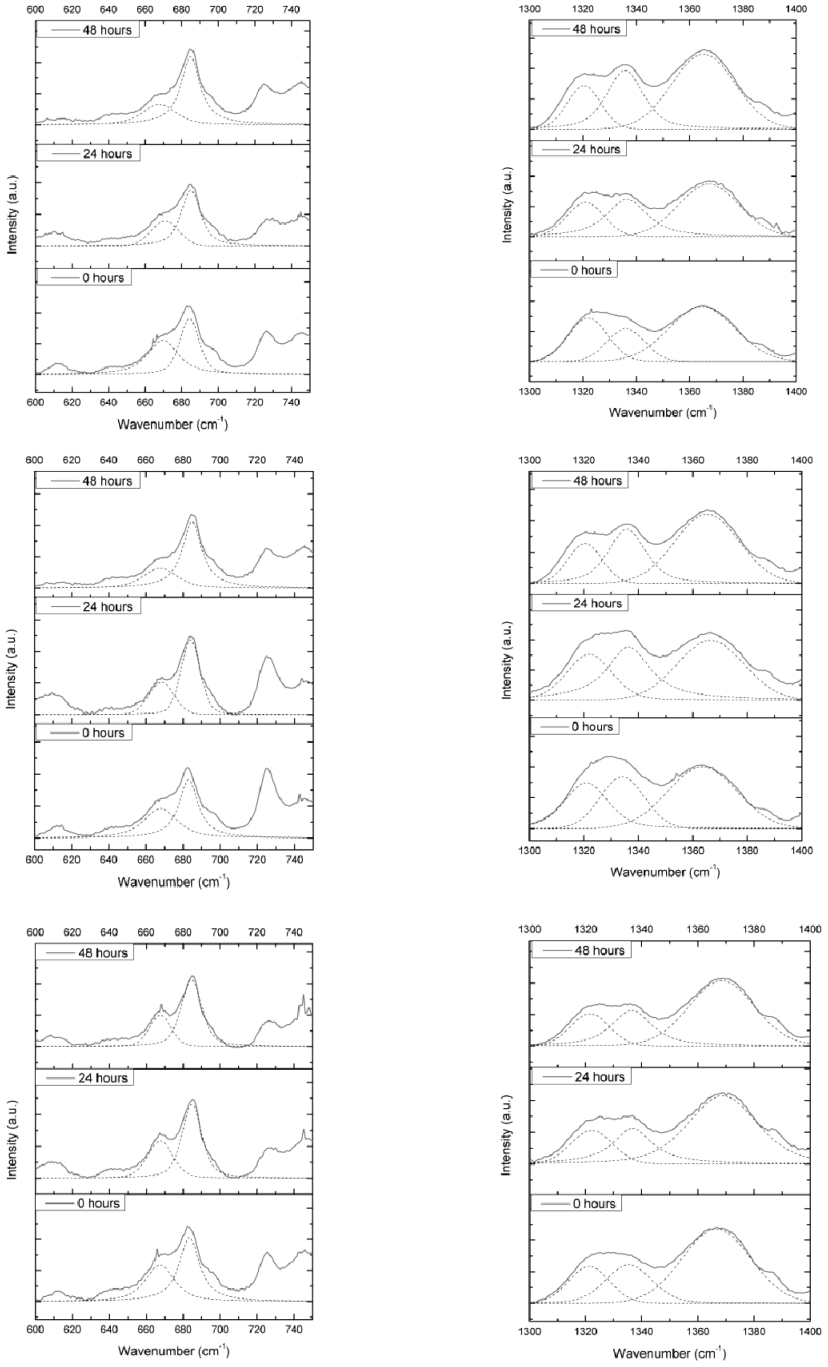

Figure 7. Monitoring the changes of the *anti* and *syn* Raman modes in the spectral regions from 600 to 740 cm^{-1} (left column) and from 1300 to 1400 cm^{-1} (right column) of H-Tel (top), Hyb-1 (middle), and Hyb-2 (bottom). All samples contained 2 mM ODNs dissolved in 10 mM Tris-HCl (pH 7.5) and either 100 mM NaCl (H-Tel) or 100 mM KCl (Hyb-1 and Hyb-2).

presence of 100 mM NaCl are also consistent with a structural change (Figure 7).

At the lower concentration of H-Tel (20 μM), its CD spectrum is consistent with previously published data and is ascribed to the basket topology of an antiparallel monomolecular G-quadruplex.[44] In the millimolar range, H-Tel shows a propensity to form what appears to be a parallel-stranded structure. We measured the CD signal at 258 nm as a function of time at different concentrations of H-Tel. The relaxations we observed were best fit by two exponentials with approximately equal amplitudes. The longer of the two relaxations was greater than 10000 s at the lowest concentration. At the highest concentration we studied, 7 mM strands, the data were fit to a single exponential. The relaxation times exhibited a very strong concentration dependence, changing by an order of magnitude over the very limited concentration range we could investigate. Thus, the CD signal arises from a multimolecular process; however, the concentration range accessible to us was insufficient for determination of the order of the reaction. Because of the presence of the shoulder around the 290 nm in the CD spectrum, at equilibrium the solution may contain a mixture of associated G-quadruplex species. We did not determine thermal melting

dx.doi.org/10.1021/bi300689t | *Biochemistry* 2012, 51, 7357−7366

curves because of the rapid evaporation of the sample in the 0.001 cm cuvettes at high temperatures.

Upon dilution of the 2 mM ODN sample to 20 μM, we observed immediately a CD spectrum that corresponds to the typical antiparallel conformation (data not shown). The rate of this reversion was too rapid to measure accurately; consequently, we were unable to calculate the dissociation rate constant.

In contrast to the behavior of H-Tel, the spectra, and presumably the structures, of Hyb-1 and Hyb-2 did not change with ODN concentration in 100 mM KCl (Figures 3B and 4B). The Raman spectra of Hyb-1 and Hyb-2 (Figure7) do not display the time-dependent intensity changes of the *anti* and *syn* modes observed for H-Tel (Figure 7). The only readily observable spectral transformation for Hyb-1 and Hyb-2 within the 48 h time frame occurred in the presence of 1 M KCl (Figures 3A,B and 4A,B).

On the basis of our results, we propose that the non-guanine bases at the 5′ and 3′ ends of Hyb-1 and Hyb-2 that form capping structures[30] hinder the association and aggregation of these two ODNs at 100 mM KCl. Consistent with this are the observations that there is no change of the CD spectrum of either ODN in the presence of 100 mM KCl up to 48 h, and the lack of intensity changes of the *anti* and *syn* Raman modes as a function of time. We also propose that the absence of bases that could form a capping structure in the H-Tel monomolecular basket structure expedites the transition into what appears to be multimolecular structures at millimolar concentrations.

Wang and Patel have conducted a landmark structural study of H-Tel at millimolar concentrations at 7 °C using nuclear magnetic resonance spectroscopy.[21] On the basis of the extinction coefficient and UV absorption units presented in their work, the concentration of H-Tel in their experiments was between 3 and 3.9 mM. In Figure 8, we present the CD spectra of 3 mM H-Tel measured at 7 °C immediately after dissolution and after 24 h at 7 °C. The initial spectrum closely resembles the H-Tel spectra we measured at 20 μM and 25 °C. After 24 h at 7 °C, the spectrum is consistent with the existence of a mixture of conformations. We did not measure the spectrum at longer times, so we cannot assess whether the transition between these two conformations had reached equilibrium. However, on the basis of the similarity of the CD spectra of the 3 mM sample at 7 °C with the spectrum of the 20 μM sample at 25 °C, we propose that at low temperatures, the conformational transition or aggregation is sufficiently slow that only the monomolecular species are present.

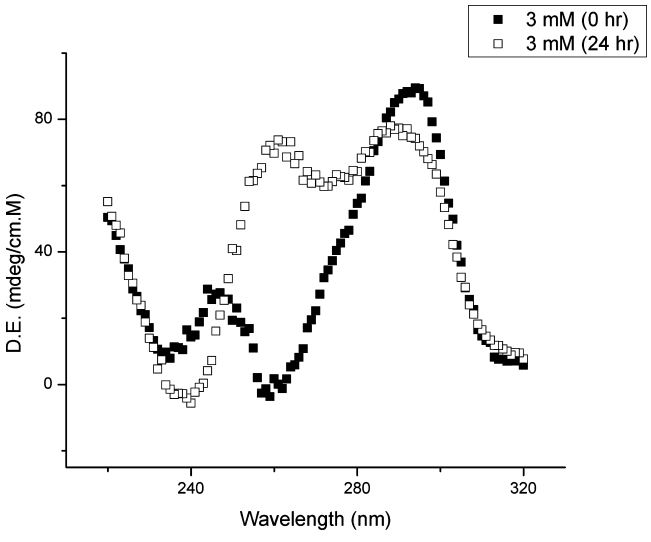

Figure 8. CD spectra of 3 mM H-Tel in 10 mM Tris-HCl (pH 7.5) with 100 mM NaCl at 7 °C after incubation for 0 (■) and 24 h (□).

The actual structure adopted at higher strand concentrations of H-Tel is unknown and is beyond the scope of this paper. However, on the basis of (1) the concentration dependence of the structural transition, (2) CD data providing a 258 nm peak, and (3) the time-dependent increase in the *anti*:*syn* ratio of the dG Raman modes of H-Tel, it appears that the predominant structure being adopted is a higher-order parallel-stranded G-quadruplex. Finally, in Figure 9, we present three possible higher-order structures that H-Tel might adopt. This schematic suggests that at millimolar strand concentrations, either the basket conformation transforms the monomeric G-quadruplexes to stack on top of each other or laterally in groups of four or the resultant structure is composed of four strands either in-register or out-of-register with respect to one another leading to the formation of higher-order G-quadruplexes. Other groups have suggested similar conformations for long repeats of the human telomeric sequence.[36,51]

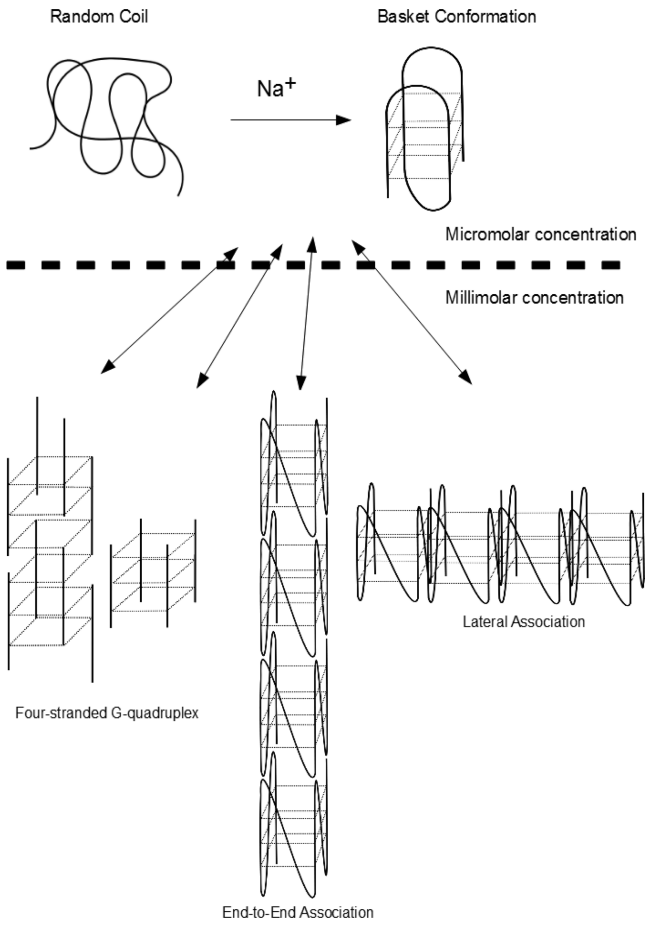

Figure 9. Schematic diagram proposing alternative configurations for the higher-order association of H-Tel monomers at high oligonucleotide concentrations.

In conclusion, our data show that at millimolar concentrations the CD spectrum of H-Tel undergoes a slow,

dx.doi.org/10.1021/bi300689t | *Biochemistry* 2012, 51, 7357−7366

concentration-dependent change. The concentration dependence means that the process is not monomolecular. The changes in the CD spectrum are rapidly reversed upon dilution of the sample. Similar changes in the spectral properties of Hyb-1 or Hyb-2 could be observed only at higher salt concentrations and higher temperatures. We have proposed a molecular mechanism involving aggregation of the folded H-Tel monomers that is consistent with our observations. We propose that the non-guanine bases at the ends of Hyb-1 and Hyb-2 inhibit the aggregation process. Further experiments ongoing in our laboratory aim to improve our understanding of this phenomenon.

AUTHOR INFORMATION

Corresponding Author

*A.S.H.: Edward S. Rogers Department of Electrical and Computer Engineering, Faculty of Applied Science and Engineering, University of Toronto, 10 King's College Rd., Toronto, Ontario M5S3G4, Canada; phone, (416) 946-0199; e-mail, a.helmy@utoronto.ca. R.B.M.: Department of Pharmaceutical Sciences, Leslie Dan Faculty of Pharmacy, University of Toronto, 144 College St., Toronto, Ontario M5S3M2, Canada; phone, (416) 978-7332; e-mail, rob.macgregor@utoronto.ca.

Funding

The Natural Sciences and Engineering Council of Canada funded this research (Grant 455967).

Notes

The authors declare no competing financial interest.

ACKNOWLEDGMENTS

We thank Dr. Tigran V. Chalikian for the use of his CD spectrometer.

REFERENCES

(1) Gellert, M., Lipsett, M. N., and Davies, D. R. (1962) Helix formation by guanylic acid. *Proc. Natl. Acad. Sci. U.S.A. 48*, 2013−2018.

(2) Hazel, P., Huppert, J., Balasubramanian, S., and Neidle, S. (2004) Loop-length-dependent folding of G-quadruplexes. *J. Am. Chem. Soc. 126*, 16405−16415.

(3) Bugaut, A., and Balasubramanian, S. (2008) A sequence-independent study of the influence of short loop lengths on the stability and topology of intramolecular DNA G-quadruplexes. *Biochemistry 47*, 689−697.

(4) Risitano, A., and Fox, K. R. (2004) Influence of loop size on the stability of intramolecular DNA quadruplexes. *Nucleic Acids Res. 32*, 2598−2606.

(5) Guo, Q., Lu, M., and Kallenbach, N. R. (1993) Effect of thymine tract length on the structure and stability of model telomeric sequences. *Biochemistry 32*, 3596−3603.

(6) Guedin, A., Alberti, P., and Mergny, J. L. (2009) Stability of intramolecular quadruplexes: Sequence effects in the central loop. *Nucleic Acids Res. 37*, 5559−5567.

(7) Guedin, A., Gros, J., Alberti, P., and Mergny, J. L. (2010) How long is too long? Effects of loop size on G-quadruplex stability. *Nucleic Acids Res. 38*, 7858−7868.

(8) Crnugelj, M., Sket, P., and Plavec, J. (2003) Small change in a G-rich sequence, a dramatic change in topology: New dimeric G-quadruplex folding motif with unique loop orientations. *J. Am. Chem. Soc. 125*, 7866−7871.

(9) Tang, C. F., and Shafer, R. H. (2006) Engineering the quadruplex fold: Nucleoside conformation determines both folding topology and molecularity in guanine quadruplexes. *J. Am. Chem. Soc. 128*, 5966−5973.

(10) Rachwal, P. A., Brown, T., and Fox, K. R. (2007) Effect of G-tract length on the topology and stability of intramolecular DNA quadruplexes. *Biochemistry 46*, 3036−3044.

(11) Sen, D., and Gilbert, W. (1990) A Sodium-Potassium Switch in the Formation of 4-Stranded G4-Dna. *Nature 344*, 410−414.

(12) Miura, T., Benevides, J. M., and Thomas, G. J., Jr. (1995) A phase diagram for sodium and potassium ion control of polymorphism in telomeric DNA. *J. Mol. Biol. 248*, 233−238.

(13) Nielsen, M. C., and Ulven, T. (2010) Macrocyclic G-quadruplex ligands. *Curr. Med. Chem. 17*, 3438−3448.

(14) Miller, M. C., Buscaglia, R., Chaires, J. B., Lane, A. N., and Trent, J. O. (2010) Hydration Is a Major Determinant of the G-Quadruplex Stability and Conformation of the Human Telomere 3′ Sequence of $d(AG_3(TTAG_3)_3)$. *J. Am. Chem. Soc. 132*, 17105−17107.

(15) Fan, H. Y., Shek, Y. L., Amiri, A., Dubins, D. N., Heerklotz, H., Macgregor, R. B., Jr., and Chalikian, T. V. (2011) Volumetric characterization of sodium-induced G-quadruplex formation. *J. Am. Chem. Soc. 133*, 4518−4526.

(16) Lane, A. N., Chaires, J. B., Gray, R. D., and Trent, J. O. (2008) Stability and kinetics of G-quadruplex structures. *Nucleic Acids Res. 36*, 5482−5515.

(17) Viglasky, V., Bauer, L., and Tluckova, K. (2010) Structural features of intra- and intermolecular G-quadruplexes derived from telomeric repeats. *Biochemistry 49*, 2110−2120.

(18) Krishnan-Ghosh, Y., Liu, D., and Balasubramanian, S. (2004) Formation of an interlocked quadruplex dimer by d(GGGT). *J. Am. Chem. Soc. 126*, 11009−11016.

(19) Marsh, T. C., and Henderson, E. (1994) G-Wires: Self-Assembly of a Telomeric Oligonucleotide, d(GGGGTTGGGG), into Large Superstructures. *Biochemistry 33*, 10718−10724.

(20) Poon, K., and Macgregor, R. B., Jr. (2000) Formation and structural determinants of multi-stranded guanine-rich DNA complexes. *Biophys. Chem. 84*, 205−216.

(21) Wang, Y., and Patel, D. J. (1993) Solution structure of the human telomeric repeat $d[AG_3(T_2AG_3)_3]$ G-tetraplex. *Structure 1*, 263−282.

(22) Parkinson, G. N., Lee, M. P., and Neidle, S. (2002) Crystal structure of parallel quadruplexes from human telomeric DNA. *Nature 417*, 876−880.

(23) Redon, S., Bombard, S., Elizondo-Riojas, M. A., and Chottard, J. C. (2003) Platinum cross-linking of adenines and guanines on the quadruplex structures of the AG3(T2AG3)3 and (T2AG3)4 human telomere sequences in Na^+ and K^+ solutions. *Nucleic Acids Res. 31*, 1605−1613.

(24) He, Y., Neumann, R. D., and Panyutin, I. G. (2004) Intramolecular quadruplex conformation of human telomeric DNA assessed with ^{125}I-radioprobing. *Nucleic Acids Res. 32*, 5359−5367.

(25) Ourliac-Garnier, I., Elizondo-Riojas, M. A., Redon, S., Farrell, N. P., and Bombard, S. (2005) Cross-links of quadruplex structures from human telomeric DNA by dinuclear platinum complexes show the flexibility of both structures. *Biochemistry 44*, 10620−10634.

(26) Li, J., Correia, J. J., Wang, L., Trent, J. O., and Chaires, J. B. (2005) Not so crystal clear: The structure of the human telomere G-quadruplex in solution differs from that present in a crystal. *Nucleic Acids Res. 33*, 4649−4659.

(27) Ying, L., Green, J. J., Li, H., Klenerman, D., and Balasubramanian, S. (2003) Studies on the structure and dynamics of the human telomeric G quadruplex by single-molecule fluorescence resonance energy transfer. *Proc. Natl. Acad. Sci. U.S.A. 100*, 14629−14634.

(28) Dai, J., Carver, M., and Yang, D. (2008) Polymorphism of human telomeric quadruplex structures. *Biochimie 90*, 1172−1183.

(29) Ambrus, A., Chen, D., Dai, J., Bialis, T., Jones, R. A., and Yang, D. (2006) Human telomeric sequence forms a hybrid-type intramolecular G-quadruplex structure with mixed parallel/antiparallel strands in potassium solution. *Nucleic Acids Res. 34*, 2723−2735.

(30) Dai, J., Carver, M., Punchihewa, C., Jones, R. A., and Yang, D. (2007) Structure of the Hybrid-2 type intramolecular human telomeric

G-quadruplex in K^+ solution: Insights into structure polymorphism of the human telomeric sequence. *Nucleic Acids Res. 35*, 4927−4940.
(31) Luu, K. N., Phan, A. T., Kuryavyi, V., Lacroix, L., and Patel, D. J. (2006) Structure of the human telomere in K^+ solution: An intramolecular (3 + 1) G-quadruplex scaffold. *J. Am. Chem. Soc. 128*, 9963−9970.
(32) Phan, A. T., Luu, K. N., and Patel, D. J. (2006) Different loop arrangements of intramolecular human telomeric (3 + 1) G-quadruplexes in K^+ solution. *Nucleic Acids Res. 34*, 5715−5719.
(33) Xu, Y., Noguchi, Y., and Sugiyama, H. (2006) The new models of the human telomere d[AGGG(TTAGGG)$_3$] in K^+ solution. *Bioorg. Med. Chem. 14*, 5584−5591.
(34) Dai, J., Punchihewa, C., Ambrus, A., Chen, D., Jones, R. A., and Yang, D. (2007) Structure of the intramolecular human telomeric G-quadruplex in potassium solution: A novel adenine triple formation. *Nucleic Acids Res. 35*, 2440−2450.
(35) Lim, K. W., Amrane, S., Bouaziz, S., Xu, W., Mu, Y., Patel, D. J., Luu, K. N., and Phan, A. T. (2009) Structure of the human telomere in K^+ solution: A stable basket-type G-quadruplex with only two G-tetrad layers. *J. Am. Chem. Soc. 131*, 4301−4309.
(36) Renciuk, D., Kejnovska, I., Skolakova, P., Bednarova, K., Motlova, J., and Vorlickova, M. (2009) Arrangements of human telomere DNA quadruplex in physiologically relevant K^+ solutions. *Nucleic Acids Res. 37*, 6625−6634.
(37) Abu-Ghazalah, R. M., Irizar, J., Helmy, A. S., and Macgregor, R. B., Jr. (2010) A study of the interactions that stabilize DNA frayed wires. *Biophys. Chem. 147*, 123−129.
(38) Cantor, C. R., Warshaw, M. M., and Shapiro, H. (1970) Oligonucleotide Interactions. 3. Circular Dichroism Studies of Conformation of Deoxyoligonucleotides. *Biopolymers 9*, 1059−1077.
(39) Irizar, J., Dinglasan, J., Goh, B., Khetani, A., Anis, H., Anderson, D., Goh, C., and Helmy, A. S. (2008) Raman Spectroscopy of Nanoparticles Using Hollow-Core Photonic Crystal Fibers. *IEEE J. Sel. Top. Quantum Electron. 14*, 1214−1222.
(40) Cregan, R. F., Mangan, B. J., Knight, J. C., Birks, T. A., Russell, P. S., Roberts, P. J., and Allan, D. C. (1999) Single-mode photonic band gap guidance of light in air. *Science 285*, 1537−1539.
(41) Laughlan, G., Murchie, A. I., Norman, D. G., Moore, M. H., Moody, P. C., Lilley, D. M., and Luisi, B. (1994) The high-resolution crystal structure of a parallel-stranded guanine tetraplex. *Science 265*, 520−524.
(42) Phillips, K., Dauter, Z., Murchie, A. I., Lilley, D. M., and Luisi, B. (1997) The crystal structure of a parallel-stranded guanine tetraplex at 0.95 Å resolution. *J. Mol. Biol. 273*, 171−182.
(43) Paramasivan, S., Rujan, I., and Bolton, P. H. (2007) Circular dichroism of quadruplex DNAs: Applications to structure, cation effects and ligand binding. *Methods 43*, 324−331.
(44) Balagurumoorthy, P., and Brahmachari, S. K. (1994) Structure and stability of human telomeric sequence. *J. Biol. Chem. 269*, 21858−21869.
(45) Miura, T., and Thomas, G. J., Jr. (1994) Structural polymorphism of telomere DNA: Interquadruplex and duplex-quadruplex conversions probed by Raman spectroscopy. *Biochemistry 33*, 7848−7856.
(46) Krafft, C., Benevides, J. M., and Thomas, G. J. (2002) Secondary structure polymorphism in *Oxytricha nova* telomeric DNA. *Nucleic Acids Res. 30*, 3981−3991.
(47) Masiero, S., Trotta, R., Pieraccini, S., De, T. S., Perone, R., Randazzo, A., and Spada, G. P. (2010) A non-empirical chromophoric interpretation of CD spectra of DNA G-quadruplex structures. *Org. Biomol. Chem. 8*, 2683−2692.
(48) Gray, D. M., Wen, J. D., Gray, C. W., Repges, R., Repges, C., Raabe, G., and Fleischhauer, J. (2008) Measured and calculated CD spectra of G-quartets stacked with the same or opposite polarities. *Chirality 20*, 431−440.
(49) Bishop, G. R., and Chaires, J. B. (2003) Characterization of DNA structures by circular dichroism. *Current Protocols in Nucleic Acid Chemistry*, Chapter 7, Unit 7.11, Wiley, New York.
(50) Neidle, S., and Balasubramanian, S. (2006) *Quadruplex nucleic acids*, Royal Society of Chemistry, Cambridge, U.K.
(51) Petraccone, L., Spink, C., Trent, J. O., Garbett, N. C., Mekmaysy, C. S., Giancola, C., and Chaires, J. B. (2011) Structure and stability of higher-order human telomeric quadruplexes. *J. Am. Chem. Soc. 133*, 20951−20961.